Microscopic derivation of superconductor-insulator boundary conditions for Ginzburg-Landau theory revisited: Enhanced superconductivity at boundaries with and without magnetic field

Albert Samoilenka and Egor Babaev
Department of Physics, KTH-Royal Institute of Technology, SE-10691, Stockholm, Sweden

Using the standard Bardeen-Cooper-Schrieffer (BCS) theory, we revise microscopic derivation of the superconductor-insulator boundary conditions for the Ginzburg-Landau (GL) model. We obtain a negative contribution to free energy in the form of surface integral. Boundary conditions for the conventional superconductor have the form $\mathbf{n} \cdot \nabla \psi = \text{const} \psi$. These are shown to follow from considering the order parameter reflected in the boundary. The boundary conditions are also derived for more general GL models with higher-order derivatives and pair-density-wave states. It shows that the boundary states with higher critical temperature and the boundary gap enhancement, found recently in BCS theory, are also present in microscopically derived GL theory. In the case of an applied external field, we show that the third critical magnetic-field value H_{c3} is higher than what follows from the de Gennes boundary conditions and is also significant in type-I regime.

I. INTRODUCTION

Superconductivity in the Ginzburg-Landau (GL) model [1] is described by a complex-valued field $\psi(\mathbf{r})$, which is called an order parameter or gap. In the bulk of the sample, ψ is found as a minimum of the free-energy functional $F_{\text{bulk}}[\psi]$. The form of this functional was microscopically derived first by Gor'kov [2]. To solve for ψ near a boundary of superconductor one has to take into account the influence of the material outside the sample. This is done by a microscopically derived boundary condition for ψ or, equivalently, by an additional surface term $F_{\text{surf}}[\psi]$ in the free-energy functional. Namely, dropping the vector potential (it is restored in Sec. VII), the free energy F of a superconductor placed in Ω is given by

$$F = F_{\text{bulk}} + F_{\text{surf}},$$

$$F_{\text{bulk}} = \int_{\Omega} d\mathbf{r}[K|\nabla\psi|^2 + \alpha|\psi|^2 + \beta|\psi|^4], \qquad (1)$$

$$F_{\text{surf}} = \gamma \int_{\partial\Omega} d\mathbf{r}_{||}|\psi|^2.$$

The order parameter is found as a minimum of F. Hence the boundary condition at $\partial\Omega$ is

$$\mathbf{n} \cdot \nabla\psi = -\frac{\gamma}{K}\psi, \qquad (2)$$

where $\mathbf{n}$ is unit vector pointing outside of the sample.

We begin by reviewing how the value of γ changes the gap behavior near the boundary in different systems. A calculation by de Gennes [3,4] gave $\gamma > 0$ at a boundary between a superconductor and a normal metal. Hence superconductivity is suppressed near such a boundary. One also defines the extension length $\Lambda = K/\gamma > 0$, which controls the range of induced superconducting correlation in the metal. On the other hand when $\gamma < 0$ superconductivity is enhanced. Such a situation is realized in several cases. Namely, for a contact with a superconductor with a higher critical temperature [5], for a local increase of electron-phonon coupling constants near the surface [6] and for superconductivity on twinning planes [7,8]. A phenomenological model with $\gamma < 0$ was analyzed in a number of works, see, e.g., Refs. [5,7,9–14]. Boundary conditions for the interface between superconductor and insulator were studied microscopically in Refs. [3,4,15,16], yielding the conclusion that it is a good approximation to set $\gamma = 0$. We will call the corresponding boundary conditions the de Gennes boundary conditions.

However, the situation for the superconductor-insulator interface is not trivial. Namely, it was recently shown microscopically that boundaries of superconductors can have (i) higher critical temperature and (ii) the gap can be enhanced at the scale of the bulk coherence length. We call this enhancement of superconductivity[1] the *boundary state*. It was found in one-, two-, and three-dimensional superconductors in the tight-binding BCS model and for the one-dimensional continuous BCS model [19]. An earlier study of the standard three-dimensional continuous BCS model concluded

---

[1]Note that, near a superconductor-insulator boundary, the gap oscillates with period $\simeq 1/k_F$, where k_F is the Fermi momentum. Some works term the first peak of these Friedel oscillations "enhancement" [17,18], even in the case where the averaged gap is not enhanced, which corresponds to the situation where de Gennes boundary conditions apply in a GL theory. Here we mean by enhancement an increase in the gap averaged over a length scale that is much larger than $1/k_F$.

that the boundary state is absent: the averaged gap near the boundaries is neither suppressed nor enhanced [17] or weakly suppressed [18]. Coulomb repulsion-induced boundary states were reported to form in certain cases in a three-dimensional continuous model where the interaction was attractive for small energies and repulsive for higher energies [17]. Superconductivity enhancement in the form of pair-density-wave (PDW) boundary states was found in spin-imbalanced superconductors [20,21] as well.

The situation is also controversial experimentally. Evidence for a substantially enhanced superconductivity near the boundary was reported in some elemental and high-temperature superconductors, see, e.g., Refs. [5,22–30]. The enhanced surface superconductivity was also mentioned in the context of enhancement of critical temperature observed in granular elemental superconductors [31–33]. The effect was interpreted as the surface being described by a different Hamiltonian based on a conjecture of different chemical compositions, which may indeed be the case, especially in complex compounds or with enhanced phonon interaction [6,34]. However, higher critical temperature of the surface was reported also for clean elemental superconductors [28,29]. Recently the claim of direct evidence for surface superconductivity was reported using the newly developed direct probe [30]. Also, results in Ref. [35] hint for possible interpretation in terms of surface critical temperature, which indeed should, in general, depend on the orientation of the boundary relative to the crystal axes.

The results from microscopic calculations and experiments show that the superconductor-insulator interface is nontrivial. This is important for various applications. For example, boundaries play a big role in quantum devices such as superconductor-based qubits and single-photon detectors, see, e.g., Refs. [36,37]. Moreover, the GL model remains the only nonlinear model amenable to the numerical solution at a substantially large length scale, required for modeling such devices. The latter provides additional motivation for this work to revise the derivation of boundary conditions in the GL model. Additionally, we resolve the ambiguity in boundary conditions when terms of higher-order in derivatives are added, see the discussion in Ref. [21].

This paper is organized in the following way: In Sec. II we set up a microscopic BCS model, which is used to derive the GL model. In Sec. III we derive that boundary conditions can be found from the mirror reflecting the order parameter in the boundary. The surface term is neglected. In Sec. IV we microscopically obtain surface term F_{surf} for several models. The result is used in subsequent sections. In Sec. V we solve for a phase diagram that includes boundary states in the GL model for the spin imbalanced system. In Sec. VI we obtain the difference of bulk and boundary critical temperatures in the GL model Eq. (1). In Sec. VII we introduce the magnetic field and give a microscopic assessment of how $\gamma < 0$ enhances the third critical magnetic field H_{c3}.

II. THE MICROSCOPIC MODEL

Consider continuous-space fermionic theory with the BCS type local attractive interaction given by strength $V > 0$. We regularize the interaction by the Debye frequency ω_D such that

only electrons with Matsubara frequency $< \omega_D$ interact. The path integral formulation of this model is given by the action S and the partition function Z (see Chapter 6.4 in Ref. [38]):

$$S = \int_0^{\frac{1}{T}} d\tau \int_{-\infty}^{+\infty} d\mathbf{r} \left[\sum_{\sigma=\downarrow,\uparrow} a_\sigma^\dagger (\partial_\tau + \varepsilon_\sigma) a_\sigma - V a_\uparrow^\dagger a_\downarrow^\dagger a_\downarrow a_\uparrow \right],$$

$$Z = \int D[a^\dagger, a] e^{-S}, \tag{3}$$

where $a_\sigma(\tau, \mathbf{r})$, $a_\sigma^\dagger(\tau, \mathbf{r})$ are Grassmann fields that correspond to fermionic creation and annihilation operators and depend on imaginary time τ, d-dimensional space coordinates $\mathbf{r}$, and spin σ. Next, $\varepsilon_\sigma \equiv E - \mu_\sigma$, where μ_σ is the chemical potential, and T is the temperature. The single-electron energy is $E \equiv E(i\nabla)$ with $E(0) = 0$, which is $E(k) = \frac{k^2}{2m}$ for free electrons. It is assumed that E depends only on the modulus of $\mathbf{k}$ so that $E(\mathbf{k}) \equiv E(|\mathbf{k}|)$. We consider a superconductor positioned in the Ω domain and an ideal insulator positioned everywhere else. To model the insulator we assume that μ_σ is finite in Ω and $\mu_\sigma \to -\infty$ elsewhere.

We perform a Hubbard-Stratonovich transformation in the Cooper channel by introducing an auxiliary bosonic field $\Delta(\tau, \mathbf{r})$:

$$e^{V \int d\tau d\mathbf{r} a_\uparrow^\dagger a_\downarrow^\dagger a_\downarrow a_\uparrow} = \int D[\Delta^\dagger, \Delta] e^{-\int d\tau d\mathbf{r} \left[\frac{\Delta^\dagger \Delta}{V} + \Delta^\dagger a_\downarrow a_\uparrow + \Delta a_\uparrow^\dagger a_\downarrow^\dagger \right]}. \tag{4}$$

By introducing Nambu spinors $A^\dagger = (a_\uparrow^\dagger, a_\downarrow)$ and $A = \begin{pmatrix} a_\uparrow \\ a_\downarrow^\dagger \end{pmatrix}$, we rewrite the partition function as

$$Z = \int D[A^\dagger, A] D[\Delta^\dagger, \Delta] e^{-\int d\tau \int d\mathbf{r} \left[\frac{\Delta^\dagger \Delta}{V} + A^\dagger(\partial_\tau + H) A \right]}$$

$$H = \begin{pmatrix} \varepsilon_\uparrow & \Delta \\ \Delta^\dagger & -\varepsilon_\downarrow \end{pmatrix}. \tag{5}$$

Then, by performing the Berezin integral, we integrate out the fermionic degrees of freedom:

$$Z = \int D[\Delta^\dagger, \Delta] e^{-F/T},$$

$$F = -T \ln \det (\partial_\tau + H) + T \int d\tau \int d\mathbf{r} \frac{\Delta^\dagger \Delta}{V}, \tag{6}$$

where F is the free energy. Next, we make mean-field assumptions: that Δ is a classical field (does not depend on τ) and that it does not fluctuate thermally and is found as a minimum of F. In this approximation the problem simplifies:

$$\ln \det (\partial_\tau + H) = \text{Tr} \sum_n^{|\omega_n| < \omega_D} \ln (i\omega_n + H)$$

$$= \text{Tr} \sum_n \ln \left(1 + (i\omega_n + H_0)^{-1} \Lambda \right) \tag{7}$$

$$= -\sum_n \sum_{k=1}^{\infty} \frac{(-1)^k}{k} \text{Tr} \left[(G_\uparrow \Delta G_\downarrow^* \Delta^*)^k \right],$$

where Matsubara frequencies are $\omega_n = 2\pi T(n + 1/2)$ and we used

$$H_0 = \begin{pmatrix} \varepsilon_\uparrow & 0 \\ 0 & -\varepsilon_\downarrow \end{pmatrix}, \quad \Lambda = \begin{pmatrix} 0 & \Delta \\ \Delta^\dagger & 0 \end{pmatrix},$$

$$(i\omega_n + H_0)^{-1}(\mathbf{r}, \mathbf{r}') = \begin{pmatrix} G_\uparrow(\mathbf{r}, \mathbf{r}') & 0 \\ 0 & -G_\downarrow^*(\mathbf{r}, \mathbf{r}'). \end{pmatrix} \quad (8)$$

Green's functions for spin-σ electrons are determined from

$$(i\omega_n + \varepsilon_\sigma) G_\sigma(\mathbf{r}, \mathbf{r}') = \delta(\mathbf{r} - \mathbf{r}'). \quad (9)$$

Since $\mu_\sigma \to -\infty$ in the insulator, the single-electron wave functions will be zero there. This results in boundary conditions for Green's functions in the following way: for coordinate $\mathbf{r}_b$ lying on the boundary $\partial\Omega$ we get

$$G_\sigma(\mathbf{r}, \mathbf{r}_b) = G_\sigma(\mathbf{r}_b, \mathbf{r}) = 0. \quad (10)$$

Now let us consider $\Omega : x > 0$. In that case the Green's function can be obtained in the form

$$G_\sigma(\mathbf{r}, \mathbf{r}') = g_\sigma(\mathbf{r} - \mathbf{r}') - g_\sigma(\mathbf{r} - \underline{\mathbf{r}}'),$$

$$g_\sigma(\mathbf{r}) = \frac{1}{(2\pi)^d} \int_{-\infty}^{+\infty} \frac{e^{i\mathbf{k}\mathbf{r}}}{i\omega_n + \varepsilon_\sigma(k)} d\mathbf{k}, \quad (11)$$

where $g_\sigma(\mathbf{r})$ is bulk Green's function, $\underline{\mathbf{r}} \equiv \mathbf{r} - 2x\hat{\mathbf{x}}$ and $k \equiv |\mathbf{k}|$.

Below we assume the following:

$$\mu_\sigma \gg \omega_D \gg T_c \gg Qv_F, \quad (12)$$

where T_c is the critical temperature, v_F is the Fermi velocity, and we are interested in a slow-varying order parameter with momentum $|\mathbf{q}| \lesssim Q$ (this justifies the expansion in q that we do later). Close to the transition to the normal state, $\Delta \to 0$. Hence we can truncate the expansion in Δ in Eq. (7). For usual superconductors, $\mu_\uparrow = \mu_\downarrow$. We also consider a superconductor with a spin imbalance. There, GL expansion is done near the tricritical point associated with the bulk Fulde-Ferrel-Larkin-Ovchinnikov (FFLO) state [39,40] (in which case $|\mu_\uparrow - \mu_\downarrow|$ is of the order of T_c).

Combining Eqs. (6) and (7) we obtain the quadratic-in-Δ part of the free energy:

$$F_2 = \int_\Omega d\mathbf{r} \frac{|\Delta|^2}{V}$$
$$- T \sum_n^{|\omega_n| < \omega_D} \int_\Omega d\mathbf{r} d\mathbf{r}' G_\uparrow(\mathbf{r}, \mathbf{r}') \Delta(\mathbf{r}') G_\downarrow^*(\mathbf{r}', \mathbf{r}) \Delta^*(\mathbf{r}). \quad (13)$$

To simplify F_2 we need to perform Fourier transform. However, integrals over x in F_2 are over half space. To extend them to full space we note that

$$G_\sigma(\underline{\mathbf{r}}, \mathbf{r}') = G_\sigma(\mathbf{r}, \underline{\mathbf{r}}') = -G_\sigma(\mathbf{r}, \mathbf{r}'). \quad (14)$$

Together with defining $\Delta(\underline{\mathbf{r}}) = \Delta(\mathbf{r})$, without loss of generality, we obtain

$$F_2 = \frac{1}{2} \int_{-\infty}^{+\infty} d\mathbf{r} \frac{|\Delta|^2}{V}$$
$$- \frac{T}{4} \sum_n \int_{-\infty}^{+\infty} d\mathbf{r} d\mathbf{r}' G_\uparrow(\mathbf{r}, \mathbf{r}') \Delta(\mathbf{r}') G_\downarrow^*(\mathbf{r}', \mathbf{r}) \Delta^*(\mathbf{r}). \quad (15)$$
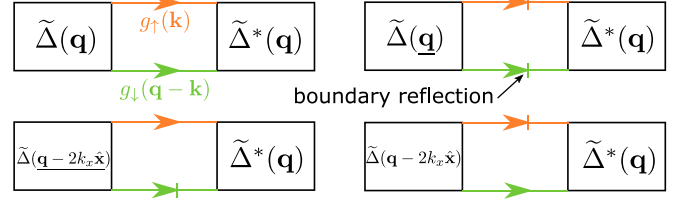

FIG. 1. Illustrations of free-energy terms which are second-order in the order parameter (16). Orange (green) lines denote bulk Green's functions of spin-up (spin-down) free electrons (reflection from the boundary is marked by a vertical line). Squares denote the order parameter Δ. In all cases, the particle-particle bubble, consisting of two Green's functions, is explicitly given by $f(k, \mathbf{k} - \mathbf{q})$, see Eq. (17). The top two diagrams with zero and two boundary reflections lead to usual bulk-like terms, where order parameters with the same momentum are coupled. They give terms proportional to $D(\mathbf{q})$ in Eq. (16). The bottom two diagrams have one reflected from the boundary electron. The latter results in coupling between order parameters of different momenta [the last term in free energy (16)]. As shown below, this gives rise to boundary states.

Performing the Fourier transform using Eq. (11) and $\Delta(\mathbf{r}) = \frac{1}{(2\pi)^d} \int_{-\infty}^{+\infty} \widetilde{\Delta}(\mathbf{q}) e^{i\mathbf{q}\cdot\mathbf{r}} d\mathbf{q}$ we obtain (see Fig. 1)

$$F_2 = \frac{1}{2} \int_{-\infty}^{+\infty} \frac{d\mathbf{q}}{(2\pi)^d} \left[\left(\frac{1}{V} - D(\mathbf{q}) \right) |\widetilde{\Delta}(\mathbf{q})|^2 \right.$$
$$\left. + \int_{-\infty}^{+\infty} \frac{d\mathbf{k}}{(2\pi)^d} \widetilde{\Delta}(\mathbf{q} - 2k_x\hat{\mathbf{x}}) \widetilde{\Delta}^*(\mathbf{q}) f(k, \mathbf{k} - \mathbf{q}) \right], \quad (16)$$

where

$$f(k, \mathbf{k} - \mathbf{q}) = T \sum_n^{|\omega_n| < \omega_D} \frac{1}{i\omega_n + \varepsilon_\uparrow(k)} \frac{1}{-i\omega_n + \varepsilon_\downarrow(\mathbf{k} - \mathbf{q})}$$

$$D(\mathbf{q}) = \int_{-\infty}^{+\infty} \frac{d\mathbf{k}}{(2\pi)^d} f(k, \mathbf{k} - \mathbf{q}). \quad (17)$$

To simplify Eq. (16) note that $f(k, \mathbf{k} - \mathbf{q})$ is not negligible[2] only at $|\varepsilon_\uparrow(k)| \lesssim \omega_D$ and $|\varepsilon_\uparrow(\mathbf{k} - \mathbf{q})| \lesssim \omega_D$. Since $|\mu_\uparrow - \mu_\downarrow| \ll \omega_D \ll \mu_\sigma$ we define $\mu = \frac{\mu_\uparrow + \mu_\downarrow}{2}$ and $h = \frac{\mu_\uparrow - \mu_\downarrow}{2}$, and hence $\varepsilon(k) = E(k) - \mu$. Then the Fermi momentum $k_F : \varepsilon(k_F) = 0$ and the Debye momentum $k_D : |\varepsilon(k_F \pm k_D)| \lesssim \omega_D$, which can be estimated as $k_D \simeq \omega_D/v_F$, where the Fermi velocity $v_F = E'(k_F)$. Hence, $f(k, \mathbf{k} - \mathbf{q})$ is nonzero when k and $\mathbf{k} - \mathbf{q}$ are on a Fermi sphere of radius k_F and thickness $2k_D$.

Usually it is assumed that Δ varies slowly with momentum $q \lesssim Q \ll k_D$ [Eq. (12)]. However, this is true only for directions parallel to the boundary. By contrast, in the x direction, fast oscillations with $q \lesssim 2k_F$ are present, the gap

---

[2]Explicitly for $\omega_D \gg T$ we obtain

$$f(k, k') \simeq \frac{\pi \left(\tanh \frac{\varepsilon_\uparrow}{2T} + \tanh \frac{\varepsilon_\downarrow'}{2T} \right) - 2 \left(\arctan \frac{\varepsilon_\uparrow}{\omega_D} + \arctan \frac{\varepsilon_\downarrow'}{\omega_D} \right)}{2\pi (\varepsilon_\uparrow + \varepsilon_\downarrow')}.$$

Note that, equivalently, we could have defined ω_D cutoff for energies $|\varepsilon| < \omega_D$ and let the sum over Matsubara frequencies be unrestricted.
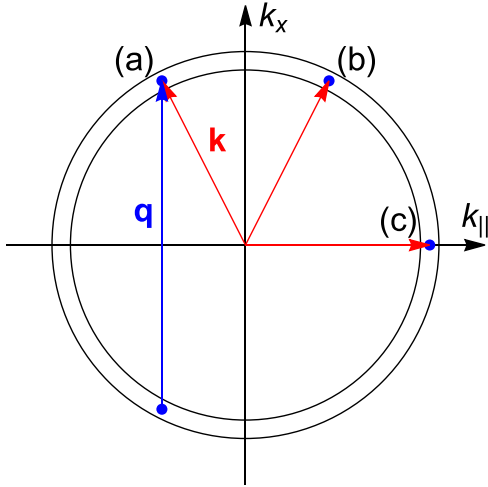
FIG. 2. Fermi sphere and three types of configurations of momenta (a)–(c) that give rise to boundary states. In all these cases, particle-particle bubble $f(k, \mathbf{k} - \mathbf{q})$ [defined by Eq. (17)] is large. This is due to the fact that $\mathbf{q}$ (blue) and $\mathbf{k}$ (red) lie in the Fermi sphere (black circles). In all cases, $|\mathbf{k}| - k_F \in [-k_D, k_D]$. By k_x we denote momentum orthogonal to the boundary and by $k_\parallel$ momentum parallel to it. Configurations can be described by the following values of k_x and $\mathbf{q}$: (a) $|k_x| \gg k_D$ and $\mathbf{q}$ is large. Namely, $|\mathbf{q} - 2k_x \hat{\mathbf{x}}| \lesssim Q$. (b) $|k_x| \gg k_D$ and $|\mathbf{q}| \lesssim Q$. (c) $|k_x| \lesssim k_D$ and $|\mathbf{q}| \lesssim Q$. Note that, for two- and three-dimensional systems, all three cases appear, whereas for one-dimensional systems, only cases (a) and (b) appear with $k_\parallel = 0$.

exhibits Friedel oscillations [17,19]. The existence of oscillations means that $f(k, \mathbf{k} - \mathbf{q})$ has contributions from three different types of points on Fermi sphere illustrated in Fig. 2.

In this work, we are interested in the description of the boundary of a superconductor at the level of the GL model. In the GL approximation, the order-parameter field is coarse-grained and thus varies slowly in real space, which corresponds to small momentum $|\mathbf{q}| \lesssim Q$; below it is denoted by $\widetilde{\psi}(\mathbf{q}) \equiv \widetilde{\Delta}(\mathbf{q})$. Whereas the order parameter that changes fast in the x direction (large momenta $Q \lesssim |q_x| \lesssim 2k_F$) we denote $\widetilde{\psi}_f(\mathbf{q}) \equiv \widetilde{\Delta}(\mathbf{q})$.

III. SMALL-q CONTRIBUTION TO BOUNDARY CONDITIONS: THE DE GENNES APPROXIMATION

We begin by reproducing the de Gennes microscopic boundary conditions under an approximation similar to that used in Refs. [3,4,15,16] considering the small-q contribution to Eq. (16). That is, in this section, we consider only the contribution from a slowly varying order parameter ψ. In this approximation we restrict $|\mathbf{q}| < Q$ in $\widetilde{\Delta}(\mathbf{q})$. Then we obtain

$$F_2^0 \simeq \frac{1}{2} \int_{-Q}^{+Q} \frac{d\mathbf{q}}{(2\pi)^d} \left(\frac{1}{V} - D(\mathbf{q}) \right) |\widetilde{\psi}(\mathbf{q})|^2. \quad (18)$$

Since $\mathbf{q}$ is small in Eq. (12), we expand $D(\mathbf{q})$ as

$$F_2^0 \simeq \int_{-Q}^{+Q} \frac{d\mathbf{q}}{(2\pi)^d} |\widetilde{\psi}(\mathbf{q})|^2 [c_0 + c_2 q^2 + c_4 q^4 + \cdots], \quad (19)$$

where c_i are the usual bulk coefficients [41]. Here we carry out the calculation in a more general form that is also applicable for the case where one has to keep higher-order derivative terms, such as the case of spin-imbalanced superconductors, including those in the FFLO state [42,43]. Transforming Eq. (19) into real space gives

$$F_{2G}^0 \simeq \int_{-\infty}^{+\infty} d\mathbf{r} [c_0 |\psi|^2 + c_2 |\nabla \psi|^2 + c_4 |\nabla^2 \psi|^2 + \cdots] \quad (20)$$

where terms with derivatives can be written in *any* integrated-by-parts form like $-c_2 \psi \nabla^2 \psi^* + c_2 \psi \nabla^4 \psi^* + \cdots$. This is possible since integral over x in Eq. (20) is over $(-\infty, +\infty)$ with ψ reflected in the boundary as $\psi(\underline{\mathbf{r}}) = \psi(\mathbf{r})$. Hence when going back to the actual system $\Omega : x > 0$ one obtains boundary conditions at $x = 0$, which depend on the chosen form of c_i terms.

For example, if the c_4 term is not included, the c_2 term gives the usual [3,4,15,16]

$$\mathbf{n} \cdot \nabla \psi = 0. \quad (21)$$

This is the de Gennes boundary condition. Applying it dictates that the critical temperature of bulk and boundaries are identical. To derive it, note that ψ is continuous across $x = 0$ but not necessarily smooth. Hence, writing $c_2 |\nabla \psi|^2$ has no additional terms at the surface and boundary conditions (21) are obtained by variation, as usual. Alternatively we could have picked $-c_2 \psi^* \nabla^2 \psi$. In that case

$$\nabla^2 \psi = 2\delta(x) \partial_x \psi|_{x \to 0^+} + \nabla^2 \psi|_{x>0}. \quad (22)$$

Integrating by parts we obtain again $c_2 |\nabla \psi|^2$, since the δ function in Eq. (22) compensates for integration by parts.

Consider now the case where the c_4 term is included, such as, for example, in the GL model of a spin-imbalanced uniform and FFLO systems [42,43]. Then $c_4 |\nabla^2 \psi|^2$ with Eq. (22) shows that, in order for energy to be finite, we need first of the two boundary conditions:

$$\mathbf{n} \cdot \nabla \psi = 0, \quad \mathbf{n} \cdot \nabla^3 \psi = 0, \quad (23)$$

where the second boundary condition is obtained from variation of the energy.

This provides microscopically derived boundary conditions in the de Gennes approximation for moderately spin-imbalanced systems and FFLO systems. Boundary conditions (23) were used before for these systems, see, e.g., Refs. [44,45]. Note that these boundary conditions eliminate the PDW boundary states discussed in Refs. [20,21] and contradict the phenomenological GL boundary conditions used there. At the same time, the PDW boundary states are unambiguously demonstrated in the full microscopic model [21]. We resolve that question below.

Note that this boundary condition of the order parameter being reflected, $\Delta(\underline{\mathbf{r}}) = \Delta(\mathbf{r})$, follows from the general property of the Green's function [Eq. (14)]. Hence it is easy to generalize it to different systems. For example, in noncentrosymmetric superconductors [46] with local interaction (3), the analog of Eq. (13) just has a matrix G and Δ [47], while the property (14) follows from the boundary condition for the Green's function [Eq. (10)]. Hence the counterpart of de Gennes boundary conditions, in that case, is obtained from

reflecting the fields at the boundary as well. For the simplest model, they are equivalent to boundary conditions obtained from variation of the free-energy function, see Ref. [47].

To summarize this section: we reported generalized to GL models with higher-derivatives derivation of de Gennes boundary conditions. However, these conditions do not reproduce the superconducting boundary states. On the other hand, it was shown microscopically that these states exist on the macroscopic length scale [21] and hence they should be reproducible in microscopically derived GL models. This problem is resolved in the next section.

IV. THE BOUNDARY CONDITIONS BEYOND THE DE GENNES APPROXIMATION

In this section, we consider whether there is a nonvanishing contribution from the terms in Eq. (16) coming from an averaging of the fast-oscillating order parameter. We denote them F_2^1 such that $F_2 = F_2^0 + F_2^1$. These terms have a large-$\mathbf{q}$ counterpart of F_2^0 [Eq. (19)] and (a), (b), (c) parts of F_2, see Fig. 2:

$$
\begin{aligned}
F_2^1 \simeq &\frac{1}{2} \int_{-Q}^{+Q} \frac{d\mathbf{q}_{||}}{(2\pi)^{d-1}} \int' \frac{dq_x}{2\pi} \left(\frac{1}{V} - D(\mathbf{q}) \right) \left| \widetilde{\psi}_f(\mathbf{q}) \right|^2 \\
&+ \frac{1}{2} \int_{-Q}^{+Q} \frac{d\mathbf{q}}{(2\pi)^d} \Bigg[\int_{-Q'}^{+Q'} \frac{dk_x}{2\pi} \widetilde{\psi}(\mathbf{q} - 2k_x\hat{\mathbf{x}}) \widetilde{\psi}^*(\mathbf{q}) \\
&\times f_1(k_x, k_x - q_x) \\
&+ \int' \frac{dk_x}{2\pi} \widetilde{\psi}_f(\mathbf{q} - 2k_x\hat{\mathbf{x}}) \widetilde{\psi}^*(\mathbf{q}) f_1(k_x, k_x) \\
&+ \int' \frac{dk_x}{2\pi} \widetilde{\psi}(\mathbf{q}) \widetilde{\psi}_f^*(\mathbf{q} - 2k_x\hat{\mathbf{x}}) f_1(k_x, k_x) \Bigg],
\end{aligned}
\tag{24}
$$

where $Q' \gtrsim Q$ and $\mathbf{q}_{||}$ are $\mathbf{q}$ components parallel to the boundary if there are any. By $\int' dp$ we denote the integral $\int_{-\infty}^{+\infty} dp$ excluding $|p| \lesssim k_D$. We define

$$
f_1(q, p) = \int_{-\infty}^{+\infty} \frac{d\mathbf{k}_{||}}{(2\pi)^{d-1}} f\left(\sqrt{q^2 + k_{||}^2}, \sqrt{p^2 + k_{||}^2} \right). \tag{25}
$$

Equation (24) is simplified to

$$
\begin{aligned}
F_2^1 \simeq &\int_{-\infty}^{+\infty} d\mathbf{r}_{||} \int' \frac{dp}{2\pi} \Bigg[\left(\frac{1}{V} - D(2p) \right) |\widetilde{\psi}_f(2p, \mathbf{r}_{||})|^2 \\
&+ \frac{1}{2} \big(\widetilde{\psi}_f(2p, \mathbf{r}_{||}) \psi^*(0, \mathbf{r}_{||}) \\
&+ \psi(0, \mathbf{r}_{||}) \widetilde{\psi}_f^*(2p, \mathbf{r}_{||}) \big) f_1(p, p) \Bigg] \\
&+ \frac{f_1(0, 0)}{4} \int_{-\infty}^{+\infty} d\mathbf{r}_{||} |\psi(0, \mathbf{r}_{||})|^2,
\end{aligned}
\tag{26}
$$

where we used $\int_{-Q}^{+Q} \frac{dq_x}{2\pi} \widetilde{\psi}(q_x, \mathbf{r}_{||}) = \psi(0, \mathbf{r}_{||})$. Note that the full field $\Delta(x)$ is zero at the boundary since electrons are perfectly reflected from it and hence Green's functions are zero there. However, the GL order parameter ψ represents only a slowly varying part of the pairing field, which can be nonzero at the boundary.

By varying Eq. (26) with respect to $\widetilde{\psi}_f$ we obtain the solution for fast-oscillating part of the order parameter:

$$
\widetilde{\psi}_f(2p, \mathbf{r}_{||}) = -\frac{\psi(0, \mathbf{r}_{||})}{2} \frac{f_1(p, p)}{\frac{1}{V} - D(2p)}. \tag{27}
$$

Inserting it back into Eq. (26), we get the surface term

$$
\begin{aligned}
F_2^1 &= \gamma \int_{-\infty}^{+\infty} d\mathbf{r}_{||} |\psi(0, \mathbf{r}_{||})|^2, \\
\gamma &= -\frac{1}{4} \left[\int' \frac{dp}{2\pi} \frac{f_1^2(p, p)}{\frac{1}{V} - D(2p)} - f_1(0, 0) \right].
\end{aligned}
\tag{28}
$$

Now let us analyze that contribution in various dimensions.

A. Superconducting wire

For one-dimensional systems, we have no contribution associated with configuration (c), see Fig. 2, in energy [Eq. (24)] and hence there should be no $f_1(0, 0)$ term in the expression for the boundary term [Eq. (28)]. However, we can use the same formula [Eq. (28)] since for $d = 1$ we have $f_1(p, q) = f(p, q)$ and hence $f_1(0, 0) = 0$. We simplify Eq. (28) as

$$
\gamma \simeq -\frac{1}{2} \int_{k_F - k_D}^{k_F + k_D} \frac{dp}{2\pi} \frac{f^2(p, p)}{\frac{1}{V} - D(2p)} \tag{29}
$$

and estimate $D(2p) \simeq \frac{N}{2}$ for $|p - k_F| \lesssim k_D$, where the density of states at the Fermi level is $N = \frac{1}{\pi v_F}$. By performing the integral over p we obtain

$$
\gamma \simeq -\frac{NV}{1 - \frac{NV}{2}} \frac{2\pi \coth\left(\frac{h}{T} \right) \mathrm{Im}\Psi^{(1)}(Z) - \mathrm{Re}\Psi^{(2)}(Z)}{32\pi^2 T}, \tag{30}
$$

where $Z = \frac{1}{2} - i\frac{h}{2\pi T}$ and $\Psi^{(n)}$ are polygamma functions of order n. For $h = 0$, Eq. (30) reduces to

$$
\gamma \simeq -\frac{NV}{1 - \frac{NV}{2}} \frac{7\zeta(3)}{8\pi^2 T}, \tag{31}
$$

where ζ is the Riemann zeta function.

Therefore, in one-dimensional GL theory, there is a boundary term for the interface between a superconductor and a vacuum [Eq. (28)]. The term has a negative microscopically derived prefactor γ. This implies that the gap is increased near the boundary and there are superconducting boundary states [19]. The conclusion applies both to quasifree and band fermions.

B. Planar superconductor

Consider the one-dimensional boundary of a two-dimensional sample. We estimate $f_1(p, p)$ for $k_F - k_D \gtrsim |p|$ as

$$
f_1(p, p) \simeq \frac{2NL}{k_F} \frac{1}{\sqrt{1 - \frac{p^2}{k_F^2}}}, \tag{32}
$$

with

$$
L = \ln \frac{\omega_D}{2\pi T} - \mathrm{Re}\Psi(Z) = \frac{1}{NV} - \frac{\alpha}{N}, \tag{33}
$$

where α is defined in Eq. (42), $T_{c1} = \frac{2e^{\gamma_E}}{\pi}\omega_D e^{-\frac{1}{NV}}$ is the bulk critical temperature, γ_E is Euler gamma, Ψ is digamma function and N is density of states at Fermi level. In this work, we consider the case of a d-dimensional system in the BCS limit where NV is small. For the two-dimensional case, $N = \frac{k_F}{2\pi v_f}$. The function $D(2p)$ for $k_F - k_D \gtrsim |p| \gtrsim k_D$ is then given by

$$D(2p) \simeq \frac{2\ln 2}{\pi} N \frac{k_D}{|p|} \frac{1}{\sqrt{1 - \frac{p^2}{k_F^2}}}. \tag{34}$$

Equations (32) and (34) allow us to compute γ in Eq. (28) up to logarithmic accuracy:

$$\gamma \simeq -\frac{\ln \frac{k_F}{k_D}}{2\pi k_F V}. \tag{35}$$

Therefore, similarly to the one-dimensional case of almost-free fermions, we recover the boundary states at the level of the GL theory.

C. Three-dimensional isotropic sample

Next we consider the two-dimensional boundary of a three-dimensional sample. In this case f_1 can be estimated as

$$f_1(p, p) \simeq \begin{cases} |p| \lesssim k_F, & \frac{\pi}{k_F} NL \\ |p| \gtrsim k_F, & 0. \end{cases} \tag{36}$$

The density of states of a three-dimensional superconductor is $N = \frac{k_F^2}{2\pi^2 v_F}$. Whereas $D(2p)$ for $k_D \lesssim |p| \lesssim k_F$ is

$$D(2p) \simeq \frac{k_D}{|p|} N \ln 2, \tag{37}$$

and $D(2p) \simeq 0$ for $|p| \gtrsim k_F$. This allows us to calculate the integral in Eq. (28), which gives:

$$\gamma \simeq \frac{\pi NL}{4k_F}\left[V\alpha + \frac{k_D}{k_F}\left(c - NV \ln 2 \ln \frac{k_F}{ck_D}\right)\right]. \tag{38}$$

Here c is the cutoff parameter of order one defined by $\int' dp = 2\int_{ck_D}^\infty dp$. Equation (38) shows that we cannot justifiably calculate γ using this analytical approach since it depends on c. Namely, as seen from Eq. (28), in our approximation, we can obtain γ only of order $f_1(0,0)$ or larger, whereas the leading-order contribution to the integral gives $\int' \frac{dp}{2\pi} \frac{f_1^2(p,p)}{\frac{1}{V} - D(2p)} \simeq f_1(0,0)$. Hence, this level of approximation indicates that γ is very small for this model: of order Eq. (38) or smaller, or could be zero. This is the property of the special case: a two-dimensional boundry of an isotropic continuous

BCS model in three dimensions. Note that the situation is different in the three-dimensional tight-binding BCS model [19].

D. The boundary states and anisotropy in three dimensions

Since many of the superconducting materials of current interest are strongly anisotropic, let us explicitly consider the effects of anisotropy. Consider the three-dimensional model that has single-electron energy $E([(k_x/a)^2 + \mathbf{k}_{||}^2]^{1/2})$, which is anisotropic for $a \neq 1$. Then γ is given by the same formula (28) with the replacement $p \to p/a$ inside the single-electron energies E. Hence, using Eq. (36) we obtain the leading-order estimate

$$\gamma \simeq -\frac{\pi(a-1)}{4k_F V}, \tag{39}$$

where k_F is the Fermi momentum parallel to the boundary. Hence, for $a > 1$, the superconductivity is enhanced near the boundary and there are boundary states. In contrast, the gap is suppressed for $a < 1$. In other words, boundary states are present if the Fermi sphere is stretched in the direction orthogonal to the boundary. Note that Ref. [35] reported a difference in T_c for samples with different orientations of the surfaces relative to crystal axes using the stiffnessometer experiment. The stifnessometer setup was proposed to resolve surface superconductivity [30].

V. BOUNDARY STATES IN SUPERCONDUCTOR WITH IMBALANCED FERMIONS

Now we consider the case where superconducting pairing takes place in a model with spin imbalance, i.e., unequal densities of spin components. In an infinite system, when there is a critical disparity of Fermi momenta of spin-up and spin-down fermionic components, the system undergoes a phase transition into an inhomogeneous FFLO state [39,40]. In such a state, the system has a modulation in the phase or modulus of the order-parameter field. At the level of the Ginzburg-Landau theory, a phase transition into such a state manifests itself through the coefficient in front of the quadratic gradient term becoming negative. Therefore, for the energy to be bounded from below, one needs to retain higher-order gradient terms with positive prefactors.

Combining the results of the microscopic derivation for bulk [42] and boundary (Sec. II), we obtain the GL model with spin imbalance:

$$F = \int_\Omega d\mathbf{r}\left\{ \alpha|\psi|^2 + K|\nabla\psi|^2 + \beta|\psi|^4 + \widetilde{K}|\nabla^2\psi|^2 + K_1|\psi\nabla\psi|^2 + \frac{K_1}{8}\left[(\psi^*\nabla\psi)^2 + (\psi\nabla\psi^*)^2\right] + \nu|\psi|^6 \right\} + \gamma\int_{\partial\Omega} d\mathbf{r}_{||}|\psi|^2. \tag{40}$$

Let us now study the problem of the boundary conditions in the presence of the higher-order derivative terms. These conditions are obtained from considering the mirror-reflected model. The condition of finiteness of energy and variation of F with respect to ψ^* gives us the boundary conditions:

$$\mathbf{n} \cdot \nabla\psi = 0, \quad \mathbf{n} \cdot \nabla^3\psi = \frac{\gamma}{\widetilde{K}}\psi, \tag{41}$$
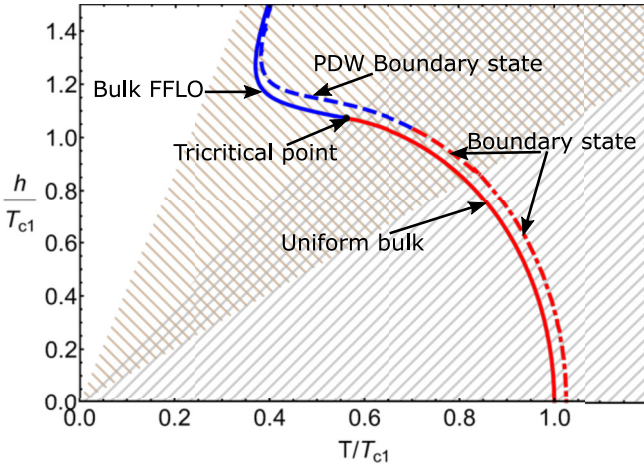
FIG. 3. Phase diagram of a two-dimensional spin-imbalanced superconductor in the GL model as a function of temperature T and spin imbalance h for $\gamma = -0.025 \frac{N v_F}{T_{c1}}$ (for example, a system in an in-plane magnetic field). Lines denote superconducting phase transitions. The bulk phase transition between normal and superconducting states is denoted by solid lines according to Eq. (44). The boundary remains superconducting for higher temperatures. The dashed lines denote a phase transition from surface superconducting to normal state according to Eq. (46) and the dot-dashed line according to Eq. (48). When the spin imbalance h is large enough, bulk and boundary states turn from sign definite (red) to periodically modulated in space states (blue). Gray hatching denotes the region where the usual GL model (1) is bounded from below (it works best for $T \to T_{c1}$ and $h \to 0$). Brown hashing shows the region where the GL model with higher-order derivatives [Eq. (40)] is convergent (the best at the tricritical point). Note that this phase diagram has a boundary PDW state extending beyond the tricritical point and there is a smooth transition to a non-PDW boundary state, which agrees with the phase diagram obtained in a Bogoliubov–de Gennes formalism [21].

where **n** is a unit vector pointing outside of the sample. Note that boundary conditions (41) differ from the phenomenological boundary conditions used in Refs. [20,21]. Whereas the de Gennes boundary conditions previously used for FFLO systems [44,45] correspond to setting $\gamma = 0$ in our boundary conditions [Eq. (41)]. We derive that γ is not zero. In Eqs. (40) and (41), γ is given by Eq. (28) while the other parameters are [42]

$$\alpha = N\left[\ln\frac{T}{T_{c1}} + \mathrm{Re}\,\Psi(Z) - \Psi(1/2)\right],$$

$$\beta = -\frac{N\mathrm{Re}\,\Psi^{(2)}(Z)}{2(4\pi T)^2}, \quad \nu = \frac{N\mathrm{Re}\,\Psi^{(4)}(Z)}{12(4\pi T)^4},$$

$$K = \frac{v_F^2 \beta}{d}, \quad \widetilde{K} = \frac{3v_F^4 \nu}{2d(d+2)}, \quad K_1 = \frac{4v_F^2 \nu}{d}. \tag{42}$$

Let us consider now the boundary physics of a spin-imbalanced superconductor. First, we determine when the superconductor transitions to a normal state. We assume that this transition is of second order and hence $\psi \to 0$ at the transition. Hence it is sufficient to solve linearized GL equations that follow from the variation of Eq. (40):

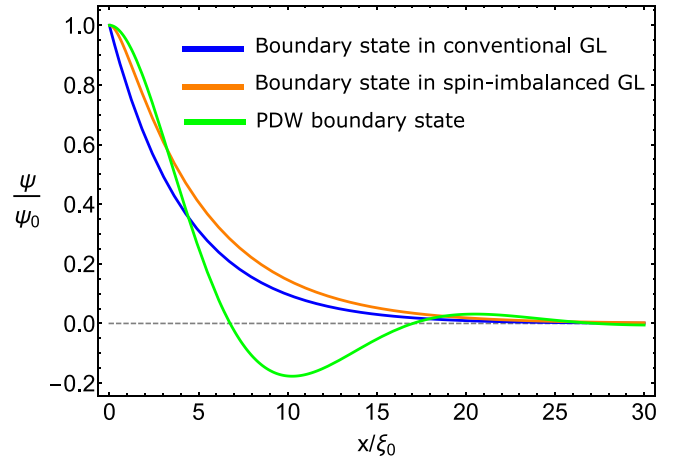$$\alpha\psi - K\nabla^2\psi + \widetilde{K}\nabla^4\psi = 0. \tag{43}$$

FIG. 4. Solutions for the boundary state in the conventional GL model (1) given by Eq. (47) (blue) and in a spin-imbalanced GL model with higher-order derivatives [Eq. (40)] given by Eq. (45) (orange). Both solutions are obtained for parameters $T/T_{c1} = 0.8$ and $h/T_{c1} \simeq 0.9$, such that they lie on the transition line in Fig. 3. The pair-density-wave (PDW) boundary-state solutions obtained in the GL model (40) given by Eq. (45) (green) at $T/T_{c1} = 0.5$ and $h/T_{c1} \simeq 1.1$. The solutions are normalized to ψ_0, which is the ψ value at the boundary and $\xi_0 = v_F\sqrt{7\zeta(3)}/(4\pi T_{c1}\sqrt{2})$.

This gives us that bulk transitions to the normal state at (see Fig. 3)

$$\text{FFLO:}\ K < 0 \quad \text{and} \quad 4\widetilde{K}\alpha = K^2,$$

$$\text{uniform:}\ K > 0 \quad \text{and} \quad \alpha = 0. \tag{44}$$

The system however has a boundary superconducting state with critical temperature which is higher than the bulk critical temperature. Let us now consider the phase transition from a superconducting boundary state to a normal state. For that matter, consider a sample positioned at $x > 0$. Then Eq. (43) should be solved together with the boundary conditions (41) and the requirement that the order parameter go to zero at infinity. We obtain the order-parameter configuration of the boundary state (see Fig. 4)

$$\psi = \text{const.} \times \left(\frac{e^{-q_+x}}{q_+} - \frac{e^{-q_-x}}{q_-}\right),$$

$$q_\pm = \sqrt{\frac{K \pm \sqrt{K^2 - 4\widetilde{K}\alpha}}{2\widetilde{K}}}, \tag{45}$$

which satisfies the second condition in Eq. (41) at the transition from the superconducting boundary to the normal state (see Fig. 3)

$$\sqrt{\widetilde{K}\alpha}(q_+ + q_-) = -\gamma. \tag{46}$$

VI. BOUNDARY STATES IN A CONVENTIONAL SUPERCONDUCTOR

Next, we consider solutions for the conventional GL model [Eq. (1)] with that derived in the above boundary conditions [Eq. (2)]. The model can be obtained from the more general expression (40) by setting $\widetilde{K} = K_1 = \nu = 0$. Hence, bulk transition from superconducting to normal state takes place at $\alpha =$

0, see Eq. (44). When the derived in the above microscopic boundary conditions are used the model exhibits superconducting boundary states. The transition from it to a normal state is obtained from the boundary conditions (2) and (43) at $\widetilde{K} = 0$. The superconducting boundary-state solution that follows from that equation is

$$\psi = \text{const.} \times e^{-q_0 x}, \quad q_0 = \sqrt{\frac{\alpha}{K}}. \tag{47}$$

Hence, transition to a normal state is given by the following condition, which corresponds to the boundary condition (2):

$$\sqrt{\alpha K} = -\gamma. \tag{48}$$

This is the GL approximation of the superconducting boundary state obtained earlier as a solution of the full microscopic theory [19]. Note that the coarse-grained GL field is smoothly varying and the enhanced pairing correlations are modeled as a source in the form of a boundary integral, yielding the boundary conditions (2). Note that this condition can be obtained from Eq. (46) by setting $\widetilde{K} \to 0$. The latter also leads to $q_- \to q_0$ and $q_+ \to (K/\widetilde{K})^{1/2}$, which means that Eq. (45) becomes Eq. (47).

From Eq. (48) we obtain that, for zero population imbalance, the boundary state transitions to normal at T_{c2} that is larger than bulk critical temperature T_{c1}:

$$\tau \equiv \frac{T_{c2} - T_{c1}}{T_{c1}} \simeq \ln \frac{T_{c2}}{T_{c1}} = \frac{\gamma^2}{NK}. \tag{49}$$

Hence, using Eq. (31) for a one-dimensional system, τ is

$$\tau \simeq \frac{7\zeta(3)}{4} \left(\frac{NV}{1 - \frac{NV}{2}} \right)^2. \tag{50}$$

For $NV \to 0$ this is equal to $\tau = \frac{7\zeta(3)}{4}(NV)^2$, which we previously obtained in a one-dimensional model without the Debye frequency [19] (note that, in Ref. [19] there is a typo and the rescaled interaction is actually $\hat{V} = NV$).

For a two-dimensional system, from Eq. (35) we obtain

$$\tau \simeq \frac{8}{7\zeta(3)} \left(\frac{T}{k_F v_F} \frac{\ln \frac{k_F}{k_D}}{NV} \right)^2. \tag{51}$$

For a three-dimensional anisotropic system with $a > 1$, we obtain from Eq. (39)

$$\tau \simeq \frac{3}{7\zeta(3)} \left(\frac{(a-1)\pi^3 T}{k_F v_F NV} \right)^2. \tag{52}$$

Analogy to wetting

As a side note, one can imagine that the plot of ψ in Fig. 4 for the usual GL model is a vertical cross-section of a tank filled with water, with ψ being the height of the surface of the water. This is not a coincidence. The energy of a thin column of water of width dx and height ψ is composed of surface-tension energy $\sigma\,dl$ and gravitational energy $\frac{\rho g}{2}\psi^2 dx$, where σ is the energy per unit surface, dl is the length of the surface, ρ is the density of water, and g is the gravitational constant. Note that we implicitly redefined $\psi \to \lambda\psi$, where λ is some dimensional constant, so that for new $[\psi] = [x]$. Then

the total energy is

$$E \simeq \text{const.} + \int_0^L dx \left[\frac{\sigma}{2} \left(\frac{d\psi}{dx} \right)^2 + \frac{\rho g}{2} \psi^2 \right], \tag{53}$$

which is similar to the GL model (1), if we substitute $\sigma \to 2K$ and $\rho g \to 2\alpha$.

Then the problem of the boundary states in a superconductor can be related to the problem of adhesion of water to a wall. In the latter case, the boundary condition is set by fixed contact angle, which is equivalent to fixing $\mathbf{n} \cdot \nabla\psi = \text{const.}$ This boundary condition is similar to Eq. (2) for a superconductor. Note that, in this analogy, the superconductor-insulator interface behaves like a hydrophilic surface. For other interfaces, like superconductor-normal metal, or an interface with certain types of different boundary layers [19], the gap can be suppressed near the boundary, which corresponds to a hydrophobic surface.

VII. H_{c3} FROM MICROSCOPICALLY DERIVED GINZBURG-LANDAU THEORY REVISITED

For conventional boundary conditions $\gamma = 0$, superconductivity in type-II materials survives near surfaces at the magnetic fields up to H_{c3}, which is higher than the critical field associated with the disappearance of superconductivity in the bulk H_{c2}. The boundary conditions that we derived have direct implications for the third critical magnetic field H_{c3}.

In the conventional picture [48] it is described by solving the linearized GL equation by using the standard de Gennes boundary conditions $\mathbf{n} \cdot \nabla\psi = 0$. Note that it has been observed earlier that numerical solution in the fully microscopic Bogoliubov-de Gennes theory (i.e., obtained beyond the quasiclassical approach) is not consistent with this picture [49] but should be more robust; however, that work did not determine H_{c3}. We are in a position now to calculate H_{c3}. Note that the problem that we will study below, namely H_{c3} in a GL model with an included surface term have been studied on phenomenological grounds in the past in the context of superconductors with modified surface layers, and superconductors with enhanced superconductivity on twinning planes [5,7,8,12]. Remarkably, enhanced H_{c3} was observed for ordinary surfaces of the elemental superconductors, and experimental papers have been explicitly raising the question of whether that originates in enhanced superconducting properties of surfaces of unknown origin [28,29]. Our goal here is to calculate H_{c3} in the microscopically derived GL theory corresponding to a regular boundary of a standard BCS superconductor.

To include magnetic field one simply replaces the derivative with a covariant derivative in Eq. (3) as $\nabla \to \nabla - ie\mathbf{A}$, where $\mathbf{A}$ is the magnetic vector potential and e is the electron charge. Next, Green's function with magnetic field G_σ^A is obtained as

$$G_\sigma^A(\mathbf{r}, \mathbf{r}') = e^{i\phi(\mathbf{r}, \mathbf{r}')} G_\sigma(\mathbf{r}, \mathbf{r}'), \tag{54}$$

where G_σ is the Green's function for zero magnetic field defined in Eq. (11) and $\phi(\mathbf{r}, \mathbf{r}') \simeq e\mathbf{A} \cdot (\mathbf{r} - \mathbf{r}')$. Note that, in this approximation, it is assumed that $\mathbf{A}$ is very slowly changing and hence it can be $\mathbf{A} \simeq \mathbf{A}(\mathbf{r})$ or $\mathbf{A} \simeq \mathbf{A}(\mathbf{r}')$ or anywhere close to $\mathbf{r}$, $\mathbf{r}'$. For details see Refs. [15,41,50]. In our calculation,

however, it is convenient to choose

$$\phi(\mathbf{r}, \mathbf{r}') \simeq e\mathbf{A}(\mathbf{r}) \cdot \mathbf{r} - e\mathbf{A}(\mathbf{r}') \cdot \mathbf{r}' \tag{55}$$

and to extend $\mathbf{A}(\underline{\mathbf{r}}) = \underline{\mathbf{A}}(\mathbf{r})$.[3]

Then property Eq. (14) is satisfied for G_σ^A as well. It means that the derivation for the model with the magnetic field is similar to the one outlined in Sec. II. The only difference is that now Δ is replaced by

$$\Delta(\mathbf{r}) \to \Delta^A(\mathbf{r}) = \Delta(\mathbf{r})e^{-2ie\mathbf{A}(\mathbf{r}) \cdot \mathbf{r}}. \tag{56}$$

Hence, for the resulting GL model, the magnetic field amounts to replacing

$$\nabla \to \nabla - 2ie\mathbf{A}. \tag{57}$$

In an external magnetic field, the boundary condition with $\gamma < 0$ leads to an increased critical magnetic field H_{c3}. It has a different dependence on temperature compared with the standard textbook derivation [48], see, for example, the phenomenological discussion in Ref. [5]. Similar observations were made in phenomenological studies of superconductors with twinning planes.

Here we compute H_{c3} with the microscopic boundary conditions derived above. Consider a two- or three-dimensional system and assume that the external magnetic field is directed along the z direction and equals H. Hence we can set a gauge for vector potential so that only nonzero component is A_y. Then the transition to the normal state is obtained by solving the linearized GL equation in terms of $\psi(x)$:

$$\alpha\psi - K\partial_x^2\psi + K(2eA_y)^2\psi = 0, \tag{58}$$

together with the boundary conditions (2). We set $A_y = (x + x_0)H$, where x_0 is to be optimized to get the highest H. Then the solution to Eq. (58) is

$$\psi = \mathrm{D}_{-\frac{1}{2}(1+\frac{\alpha}{2|e|HK})}\left((x + x_0)\sqrt{4|e|H}\right), \tag{59}$$

where $\mathrm{D}_\nu(x)$ is parabolic cylinder function. To find x_0, it is convenient to calculate the first $d\psi$ integral of Eq. (58). By using boundary conditions (2), we obtain

$$\psi^2(x_0)\left[\frac{\gamma^2 - \alpha K}{K^2} - (2eHx_0)^2\right] - \int_{x_0}^\infty [2eH\psi(x)]^2 2x\,dx = 0. \tag{60}$$

This equation sets the relation between x_0 and H, when the solution for ψ [Eq. (59)] is inserted. Since we search for the largest H, a derivative of Eq. (60) with respect to x_0 should be zero. It gives

$$x_0 = -\frac{\sqrt{\gamma^2 - \alpha K}}{2|e|HK}. \tag{61}$$

Here we picked the minus sign so that Eq. (60) can be satisfied. Next, in order to find H we can either solve Eq. (60) or the boundary condition (2). We solve the latter, which using

---

[3]Note that this extension is purely fictitious and is used just to derive the boundary conditions for Δ easily. The actual $\mathbf{A}$ has different value outside of the superconductor, which follows from the magnetic energy defined over all space, $\int_{-\infty}^{+\infty} d\mathbf{r}\frac{(\mathbf{B}-\mathbf{H})^2}{2}$, where $\mathbf{B} \equiv \nabla \times \mathbf{A}$ and $\mathbf{H}$ is the external magnetic field.
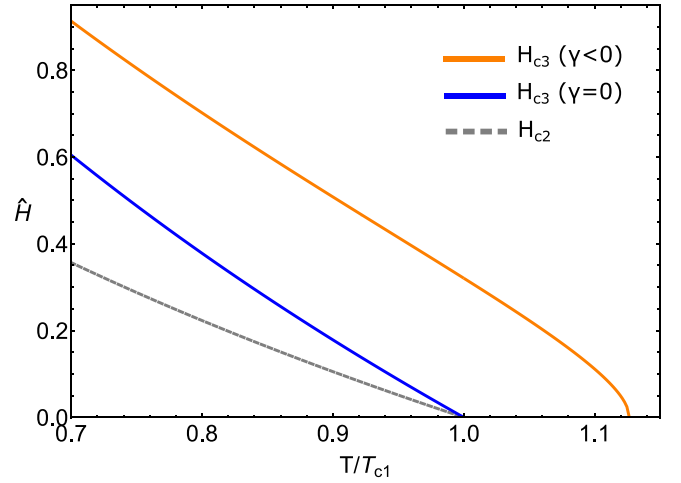

FIG. 5. Rescaled critical magnetic fields $\hat{H} \equiv \frac{2|e|K}{N}H$ as a function of temperature T. Bulk transitions to the normal state for fields higher than $H_{c2} = -\frac{\alpha}{2|e|K}$. In the derivation [48] with zero boundary term ($\gamma = 0$), the surface transitions to the normal state at higher field $H_{c3} \simeq 1.69H_{c2}$. From Eq. (62) we obtain that, if in Eq. (1) the boundary term is present with $\gamma < 0$, then surface superconductivity is enhanced and boundary transitions to normal at field H_{c3} higher than that for $\gamma = 0$. Here we have chosen $\gamma = -0.05\frac{Nv_F}{T_{c1}}$.

the expression for x_0 Eq. (61) and rescaling amounts to solving numerically for η for a given a in

$$\frac{(1 - \sqrt{a})}{\sqrt{\eta}}\mathrm{H}_{\frac{a-1-\eta}{2\eta}}\left(-\sqrt{a/\eta}\right) = \mathrm{H}_{\frac{a-1+\eta}{2\eta}}\left(-\sqrt{a/\eta}\right), \tag{62}$$

where $\mathrm{H}_\nu(x)$ is a Hermite polynomial, $a = 1 - \frac{\alpha K}{\gamma^2}$, and $\eta = \frac{2|e|HK^2}{\gamma^2}$. The H obtained then is equal to H_{c3}. See Fig. 5 for a plot of H_{c3}. The H_{c3} is, therefore, higher than in the original Saint-James de Gennes derivation [48]. Also, note that H_{c3} should exist for type-I superconductors in significant temperature range.

VIII. CONCLUSIONS

We considered the generic BCS model for spin-balanced and spin-imbalanced fermions. From that model, we derived the boundary conditions for the GL theory for the interface between a superconductor and an insulator. We showed that the free energy of a superconductor acquires an additional term given by the surface integral of $\gamma|\psi|^2$. The physical origin of this term is the fact that, near a well-reflecting boundary, the total gap oscillates with $\simeq k_F$ momentum. This oscillatory part is coupled to the averaged gap ψ in GL theory, leading to an additional surface term. We obtained that $\gamma < 0$ for one- and two-dimensional continuous BCS models. For the three-dimensional isotropic BCS model, the surface term is beyond the resolution of our analytical approach. Whereas for an anisotropic three-dimensional model we have shown that γ can be positive or negative. The negative γ leads to enhanced superconductivity near boundaries. Note that, for the tight-binding BCS model the surface superconductivity exists in all dimensions [19], which also implies boundary conditions with $\gamma < 0$.

To obtain boundary conditions we showed that the following procedure can be applied: Consider the GL model that in general has the highest in derivative term of order k. Then one should reflect the order parameter in the boundary and write the free energy as an integral over the whole space. This reflection automatically applies proper boundary conditions. Namely, one can write kinetic terms in any integrated-by-parts form and search for a minimum of the total free energy. Boundary conditions are obtained from the condition on energy to be finite and from the variation of this functional with respect to the order parameter. As a result, we obtained that usually all normal to boundary odd derivatives of ψ of order less than $k - 1$ should be zero, whereas $k - 1$ derivative will be proportional to $\gamma \psi$.

For the standard GL model with second-order derivatives, $k = 2$ and hence we obtain boundary conditions $\mathbf{n} \cdot \nabla \psi = -\frac{\gamma}{K}\psi$, see Eq. (2). The GL model for spin-imbalanced systems requires taking into account fourth-order gradient terms and hence has boundary conditions $\mathbf{n} \cdot \nabla \psi = 0$, $\mathbf{n} \cdot \nabla^3 \psi = \frac{\gamma}{K}\psi$, see Eq. (41). Using these new microscopically derived boundary conditions, we obtained superconducting boundary states in the conventional GL model and revised the calculation of PDW boundary states in the spin-imbalanced GL model.

The obtained boundary conditions allow GL theory to account, in a microscopically accurate way for boundary states that were found earlier in fully microscopic solutions of BCS theory [19]. Namely, in the GL model for $\gamma < 0$, in zero external magnetic field, the superconducting gap is larger near the surface than in the bulk, and superconductivity survives for higher temperatures. Since microscopic calculations show that superconductivity is more enhanced at the edges and corners of a three-dimensional sample, to model these effects one should add analogous extra contributions for corners and edges.

By adding an external magnetic field we revised the theory of the third critical magnetic field H_{c3} for a BCS superconductor. The surface effects make this field larger and extending in a type-I regime, compared with results obtained using de Gennes boundary conditions.

We note that these surface effects can be described in a quasiclassical approach if one augments the theory by taking into account higher-momentum contributions to the boundary conditions.

ACKNOWLEDGMENTS

[1] V. L. Ginzburg and L. D. Landau, On the Theory of Superconductivity, Zh. Eksperim. I. Teor. Fiz **20**, 1064 (1950).

[2] L. P. Gor'kov, Microscopic Derivation of the Ginzburg-Landau Equations in the Theory of Superconductivity, ZhETF 36, 1918, (1959) [Sov. Phys. JETP **36**, 1918 (1959).

[3] P. de Gennes, Boundary effects in superconductors, Rev. Mod. Phys. **36**, 225 (1964).

[4] P.-G. De Gennes, *Superconductivity of Metals and Alloys* (CRC Press, Boca Raton, 2018).

[5] H. Fink and W. Joiner, Surface Nucleation and Boundary Conditions in Superconductors, Phys. Rev. Lett. **23**, 120 (1969).

[6] V. Ginzburg, On Surface Superconductivity, Phys. Lett. **13**, 101 (1964).

[7] A. I. Buzdin and L. Bulaevskii, Localized superconductivity in NSN systems, JETP Lett. **34**, 112 (1981).

[8] I. Khlyustikov and A. Buzdin, Twinning-plane superconductivity, Adv. Phys. **36**, 271 (1987).

[9] E. A. Andryushin, V. L. Ginzburg, and A. P. Silin, Boundary conditions in the macroscopic theory of superconductivity, Phys. Usp. **36**, 854 (1993).

[10] N. Ivanov and T. Mishonov, Heat Capacity of a Thick Superconducting Plate with Proximity Effect, Tech. Rep., Joint Inst. for Nuclear Research, 1987.

[11] A. Abrikosov, A. I. Buzdin, M. Kulic, and D. Kuptsov, Thermodynamic and magnetic-properties of a system of superconducting twinning planes, Zh. Eksp. Teor. Fiz **95**, 383 (1989) [Sov. Phys. JETP **68**, 210 (1989)].

[12] V. Averin, A. I. Buzdin, and L. Bulaevskii, Theory of localized superconductivity, Zh. Eksp. Teor. Fiz **84**, 748 (1983) [Sov. Phys. JETP **57**, 426 (1983)].

[13] J. Simonin, Surface term in the superconductive Ginzburg-Landau free energy: Application to thin films, Phys. Rev. B **33**, 7830 (1986).

[14] M. Kaganov and A. Omel'Yanchuk, Phenomenological theory of phase transition in a thin ferromagnetic plate, JETP **34**, 895 (1972).

[15] A. Abrikosov, Concerning surface superconductivity in strong magnetic fields, Sov. Phys. JETP **20**, 480 (1965).

[16] C. Caroli, P. De Gennes, and J. Matricon, Sur certaines propriétés des alliages supraconducteurs non magnétiques, J. Phys. Radium **23**, 707 (1962).

[17] T. Giamarchi, M. Béal-Monod, and O. T. Valls, Onset of surface superconductivity, Phys. Rev. B **41**, 11033 (1990).

[18] B. P. Stojković and O. T. Valls, Order parameter near a superconductor-insulator interface, Phys. Rev. B **47**, 5922 (1993).

[19] A. Samoilenka and E. Babaev, Boundary states with elevated critical temperatures in Bardeen-Cooper-Schrieffer superconductors, Phys. Rev. B **101**, 134512 (2020).

[20] M. Barkman, A. Samoilenka, and E. Babaev, Surface Pair-Density-Wave Superconducting and Superfluid States, Phys. Rev. Lett. **122**, 165302 (2019).

[21] A. Samoilenka, M. Barkman, A. Benfenati, and E. Babaev, Pair-density-wave superconductivity of faces, edges, and vertices in systems with imbalanced fermions, Phys. Rev. B **101**, 054506 (2020).

[22] R. Lortz, T. Tomita, Y. Wang, A. Junod, J. Schilling, T. Masui, and S. Tajima, On the origin of the double superconducting transition in overdoped YBa$_2$Cu$_3$O$_x$, Phys. C (Amsterdam, Neth.) **434**, 194 (2006).

[23] E. Janod, A. Junod, T. Graf, K.-Q. Wang, G. Triscone, and J. Muller, Split superconducting transitions in the specific heat and magnetic susceptibility of $YBa_2Cu_3O_x$ versus oxygen content, Phys. C (Amsterdam, Neth.) **216**, 129 (1993).

[24] R. A. Butera, High-resolution heat capacity of $YBa_2Cu_3O_{6.9}$ over the superconducting transition region, Phys. Rev. B **37**, 5909 (1988).

[25] M. I. Tsindlekht, G. I. Leviev, I. Asulin, A. Sharoni, O. Millo, I. Felner, Y. B. Paderno, V. Filippov, and M. A. Belogolovskii, Tunneling and magnetic characteristics of superconducting ZrB_{12} single crystals, Phys. Rev. B **69**, 212508 (2004).

[26] M. Belogolovskii, I. Felner, and V. Shaternik, Zirconium dodecaboride, a novel superconducting material with enhanced surface characteristics, in *Boron Rich Solids* (Springer, Berlin 2010), pp. 195–206.

[27] R. Khasanov, D. Di Castro, M. Belogolovskii, Y. Paderno, V. Filippov, R. Brütsch, and H. Keller, Anomalous electron-phonon coupling probed on the surface of superconductor ZrB_{12}, Phys. Rev. B **72**, 224509 (2005).

[28] I. Khlyustikov, Critical magnetic field of surface superconductivity in lead, J. Exp. Theor. Phys. **113**, 1032 (2011).

[29] I. Khlyustikov, Surface superconductivity in lead, J. Exp. Theor. Phys. **122**, 328 (2016).

[30] I. Mangel, I. Kapon, N. Blau, K. Golubkov, N. Gavish, and A. Keren, Stiffnessometer: A magnetic-field-free superconducting stiffness meter and its application, Phys. Rev. B **102**, 024502 (2020).

[31] G. Deutscher, M. Gershenson, E. Grünbaum, and Y. Imry, Granular superconducting films, J. Vac. Sci. Technol. **10**, 697 (1973).

[32] R. W. Cohen and B. Abeles, Superconductivity in granular aluminum films, Phys. Rev. **168**, 444 (1968).

[33] R. W. Cohen, B. Abeles, and G. S. Weisbarth, Strong-coupling superconductivity in gallium, Phys. Rev. Lett. **18**, 336 (1967).

[34] D. G. Naugle, J. Baker, and R. E. Allen, Evidence for a surface-phonon contribution to thin-film superconductivity: Depression of T_c by noble-gas overlayers, Phys. Rev. B **7**, 3028 (1973).

[35] I. Kapon, Z. Salman, I. Mangel, T. Prokscha, N. Gavish, and A. Keren, Phase transition in the cuprates from a magnetic-field-free stiffness meter viewpoint, Nat. Commun. **10**, 2463 (2019).

[36] J. D. S. Bommer, H. Zhang, O. Gul, B. Nijholt, M. Wimmer, F.N. Rybakov, J. Garaud, D. Rodic, E. Babaev, M. Troyer, D. Car, S.R. Plissard, E. P. A. M. Bakkers, K. Watanabe, T. Taniguchi, and L. P. Kouwenhoven, Spin-Orbit Protection of Induced Superconductivity in Majorana Nanowires, Phys. Rev. Lett. **122**, 187702 (2019).

[37] R. Baghdadi, E. Schmidt, S. Jahani, I. Charaev, M. G. Müller, M. Colangelo, D. Zhu, K. Ilin, A. D. Semenov, Z. Jacob *et al.*, Enhancing the performance of superconducting nanowire-based detectors with high-filling factor by using variable thickness, Supercond. Sci. Technol. **34**, 035010 (2021).

[38] A. Altland and B. D. Simons, *Condensed Matter Field Theory* (Cambridge University Press, Cambridge 2010).

[39] P. Fulde and R. A. Ferrell, Superconductivity in a strong spin-exchange field, Phys. Rev. **135**, A550 (1964).

[40] A. I. Larkin and Y. N. Ovchinnikov, Nonuniform state of superconductors, Zh. Eksp. Teor. Fiz. **47**, 1136 (1964) [Sov. Phys. JETP **20**, 762 (1965)].

[41] A. A. Abrikosov, L. P. Gorkov, and I. E. Dzyaloshinski, *Methods of Quantum Field Theory in Statistical Physics* (Courier Corporation, 2012).

[42] A. I. Buzdin and H. Kachkachi, Generalized Ginzburg-Landau theory for nonuniform FFLO superconductors, Phys. Lett. A **225**, 341 (1997).

[43] L. Radzihovsky, Fluctuations and phase transitions in Larkin-Ovchinnikov liquid-crystal states of a population-imbalanced resonant Fermi gas, Phys. Rev. A **84**, 023611 (2011).

[44] K. V. Samokhin and B. P. Truong, Fulde-Ferrell-Larkin-Ovchinnikov superconductors near a surface, Phys. Rev. B **99**, 014503 (2019).

[45] V. D. Plastovets and D. Y. Vodolazov, Paramagnetic meissner, vortex, and onionlike ground states in a finite-size Fulde-Ferrell superconductor, Phys. Rev. B **101**, 184513 (2020).

[46] E. Bauer and M. Sigrist, *Non-Centrosymmetric Superconductors: Introduction and Overview* (Springer Science & Business Media, Berlin, 2012), Vol. 847.

[47] A. Samoilenka and E. Babaev, Spiral magnetic field and bound states of vortices in noncentrosymmetric superconductors, Phys. Rev. B **102**, 184517 (2020).

[48] D. Saint-James and P. G. de Gennes, Onset of superconductivity in decreasing fields, Phys. Lett. **7** (1963).

[49] R. J. Troy and A. T. Dorsey, Self-consistent microscopic theory of surface superconductivity, Phys. Rev. B **51**, 11728 (1995).

[50] L. Gor'kov, The critical supercooling field in superconductivity theory, Soviet Phys. JETP **10**, 593 (1960).